

## Computer Solutions of Plane Strain Axisymmetric Thermomechanical Problems

**Ahmet N. ERASLAN**

*Middle East Technical University, Department of Engineering Sciences  
Ankara-TURKEY*

*e-mail: aeraslan@metu.edu.tr*

**Hakan ARGESO**

*Başkent University, Department of Mechanical Engineering  
Ankara-TURKEY*

Received 27.06.2005

### Abstract

A simple computational model is developed to estimate elastic, elastic-plastic, fully plastic, and residual stress states in generalized plane strain axisymmetric structures considering temperature dependent physical properties as well as nonlinear isotropic strain hardening. Using the von Mises yield criterion, total deformation theory and a Swift-type nonlinear hardening law, a single nonlinear differential equation governing thermoelastoplastic behavior is obtained. A shooting technique using Newton iterations with numerically approximated tangents is used for the computer solution of the governing equation. Various numerical examples including plane strain and generalized plane strain problems for cylinders and tubes are handled. It is shown that the thermoelastoplastic response of the structures considered here is affected significantly by the temperature dependency of the physical properties of the material; the effect of nonlinear strain hardening, however, is observed to be not as great as the latter.

**Key words:** Stress analysis, Thermoelastoplasticity, Residual stresses, Nonlinear strain hardening, Von Mises criterion

### Introduction

Thermomechanical analysis of basic structures like rods, tubes, disks, and spherical shells is of great importance in engineering design and operation (Boley and Weiner, 1960; Timoshenko and Goodier, 1970; Johnson and Mellor, 1973; Chen and Han, 1988; Rees, 1990; Uğural and Fenster, 1995; Eraslan and Akis, 2003). Since, in general, to better utilize the material, plastic deformation may be allowed to some extent, recent studies have focused on elastic-plastic treatment of thermal behavior. The special case, in which thermal deformations are caused by a prescribed symmetrical temperature distribution or internal energy generation in systems that can be treated under plane-strain presupposition, has been the topic of numerous investigations. Examples may

be found in recent articles by Orcan and Eraslan (2001), Orcan and Gulgec (2001), Eraslan and Orcan (2002), Eraslan (2003), Eraslan et al. (2003), Eraslan and Orcan (2004), and in the references cited there.

Recently, Eraslan (2004) suggested a computational procedure for an easy-to-handle unified treatment of all types of rotating nonlinear strain hardening elastic-plastic shafts under a plane strain assumption. This computational procedure was later successfully adopted by the authors (Eraslan and Argeso, 2005a) for the computer solution of a class of plane strain thermal stress problems using constant physical properties. The verification of this model is performed comprehensively in comparison with (i) analytical solutions in the elastic range, and (ii) incremental theory using Tresca's yield criterion

available in the literature. However, it is well known that the mechanical and thermal properties of most engineering materials vary considerably with temperature. It is therefore the objective of this article to describe the extension of the work of Eraslan and Argeso (2005a) to include temperature dependent physical properties. We construct a computational model to estimate the thermoelastoplastic response of axisymmetric structures, considering nonlinear isotropic strain hardening. Empirical relations based on experimental observations describing the temperature dependency of modulus of elasticity, yield limit, thermal conductivity and coefficient of thermal expansion of high strength low alloy steel are incorporated (Orcan and Eraslan, 2001). Using the von Mises yield criterion, Henky's deformation theory, and a Swift-type nonlinear hardening law, a single nonlinear differential equation governing the thermoelastoplastic behavior of generalized plane strain problems is obtained. A nonlinear shooting technique is used for the numerical solution of the governing equation (Eraslan and Kartal, 2004; Eraslan and Argeso, 2005b).

### Computational Model

Formulations in the following sections use the notation and basic equations of thermoelasticity given in Boley and Weiner (1960).

### Physical properties

As stated earlier, the mechanical and thermal properties of most engineering materials are known to vary considerably with temperature (Boley and Weiner, 1960). Hence, to obtain more realistic predictions in thermomechanical calculations, the temperature dependency of physical properties must be taken into account. For this purpose, we consider a high-strength low-alloy steel for which the modulus of elasticity  $E$  and uniaxial yield limit  $\sigma_0$  vary with temperature  $T$  according to the empirical relations (Orcan and Eraslan, 2001)

$$E(T) = 200 \times 10^9 \left[ 1 + \frac{T}{2000 \ln(T/1100)} \right] \quad [\text{N/m}^2], \quad (1)$$

$$\sigma_0(T) = 410 \times 10^6 \left[ 1 + \frac{T}{600 \ln(T/1630)} \right] \quad [\text{N/m}^2]. \quad (2)$$

In addition, the thermal conductivity  $k$  and the coefficient of thermal expansion  $\alpha$  for the steel alloy considered can be fit in quadratic forms as

$$\begin{aligned} k &= k_0 + k_1 T + k_2 T^2 \\ &= 45 - 0.018T - 1.0 \times 10^{-5} T^2 \quad [\text{W/m}^2 \text{ } ^\circ\text{C}], \end{aligned} \quad (3)$$

$$\begin{aligned} \alpha &= \alpha_0 + \alpha_1 T + \alpha_2 T^2 \\ &= 11.7 \times 10^{-6} + 3.0 \times 10^{-9} T + 2.5 \times 10^{-12} T^2 \\ &\quad [1/^\circ\text{C}]. \end{aligned} \quad (4)$$

Variation of the nondimensional forms of the physical properties with temperature in the range  $0 - 400^\circ\text{C}$  is depicted in Figure 1. Although all properties vary with temperature to some extent, the highest impact is on the yield limit  $\sigma_0(T)$ , which is expected to affect the thermoplastic response of the structures considerably.

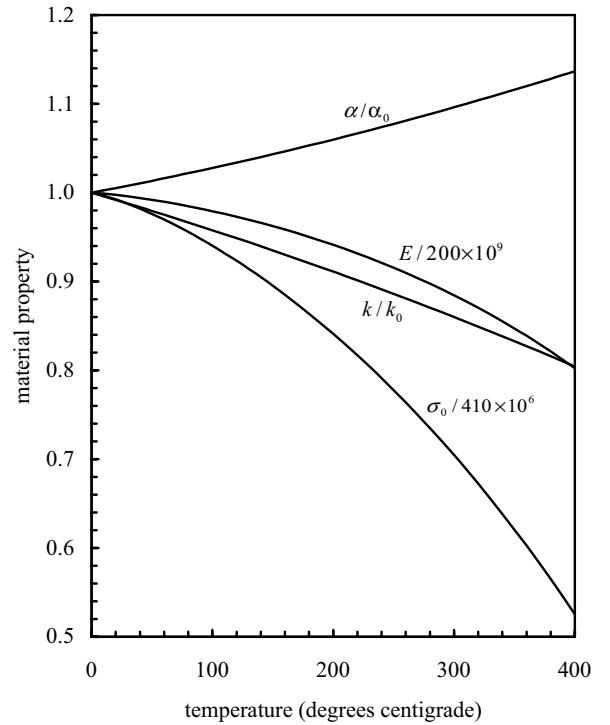


**Figure 1.** Variation of modulus of elasticity  $E$ , uniaxial yield limit  $\sigma_0$ , coefficient of thermal expansion  $\alpha$ , and thermal conductivity  $k$  with temperature for high strength low alloy steel.

### Temperature distribution

The elastoplastic model that will be developed next will be valid for any prescribed temperature distribution. However, to give some specific examples, we pay attention to long cylinders and tubes under uniform energy generation  $Q$  per unit volume-time. The temperature  $T$  in such systems is governed by the heat conduction equation

$$\frac{1}{r} \frac{d}{dr} \left( kr \frac{dT}{dr} \right) + Q = 0. \quad (5)$$

For a cylinder of outer radius  $b$  having a constant surface temperature  $T(b) = 0$ , the general solution is

$$k_0 T + \frac{k_1}{2} T^2 + \frac{k_2}{3} T^3 = \frac{Q}{4} (b^2 - r^2). \quad (6)$$

On the other hand, for a tube of inner radius  $a$  possessing boundary conditions

$$-k \frac{dT}{dr} \Big|_{r=a} = 0 \quad \text{and} \quad T(b) = 0, \quad (7)$$

the general solution becomes

$$k_0 T + \frac{k_1}{2} T^2 + \frac{k_2}{3} T^3 = \frac{Q}{4} \left[ 2a^2 \ln \left( \frac{r}{b} \right) + b^2 - r^2 \right]. \quad (8)$$

These analytical solutions are in cubic forms and assume 3 roots at any radial location. However, only one of these roots falls in the calculation domain. The others either produce negative or complex temperatures. It is noted that for constant values of thermal conductivity  $k = k_0$  Eqs. (6) and (8) reduce respectively to

$$k_0 T = \frac{Q}{4} (b^2 - r^2), \quad (9)$$

$$k_0 T = \frac{Q}{4} \left[ 2a^2 \ln \left( \frac{r}{b} \right) + b^2 - r^2 \right], \quad (10)$$

which have been used in thermoelastoplastic calculations by Orcan (1994) and Orcan and Gulgec (2001).

It is now appropriate to introduce the following dimensionless and normalized variables based on the physical properties at a reference temperature  $T_0$ . Radial coordinate:  $\bar{r} = r/b$ , normal stress:  $\bar{\sigma}_j = \sigma_j/\sigma_0(T_0)$  normal strain:  $\bar{\epsilon}_j = \epsilon_j E(T_0)/\sigma_0(T_0)$ , radial displacement:  $\bar{u} = uE(T_0)/\sigma_0(T_0)b$ , heat load:  $\bar{Q} = QE(T_0)\alpha(T_0)b^2/\sigma_0(T_0)k(T_0)$ , the coefficient of

thermal expansion:  $\bar{\alpha} = \alpha E(T_0)/\sigma_0(T_0)$ , hardening parameter:  $H = \eta\sigma_0(T_0)/E(T_0)$ , modulus of elasticity:  $\bar{E} = E/E(T_0)$ , and uniaxial yield limit:  $\bar{\sigma}_0 = \sigma_0/\sigma_0(T_0)$  with  $\eta$  being the hardening parameter.

Taking  $T_0 = 0$  and assigning  $\bar{Q} = 6.1$  the distributions of temperature as well as temperature gradient in a long cylinder are calculated and plotted in Figure 2(a). In this figure, solid lines show the results of temperature dependent thermal conductivity calculations by the use of Eq. (6), while dashed lines show constant property results obtained by the use of Eq. (9). The temperature and temperature gradient profiles in a long tube of inner radius  $\bar{a} = a/b = 0.4$  are presented in Figure 2(b). The parameters used in drawing this figure are  $T_0 = 0$  and  $\bar{Q} = 10$ . The solid lines in Figure 2(b) are based on the results of Eq. (8) and the dashed lines on Eq. (10). The effect of temperature dependent thermal conductivity on the thermal response of a uniform heat generating cylinder and of a uniform heat generating tube can clearly be evaluated in Figures 2(a) and (b), respectively.

### The governing equation

The equations given below are written in terms of the nondimensional variables defined above. For convenience, overbars are dropped. A state of generalized plane strain and small deformations are presumed. The strain displacement relations:  $\epsilon_r = u'$ ,  $\epsilon_\theta = u/r$ , the equation of equilibrium in radial direction

$$\sigma_\theta = (r\sigma_r)', \quad (11)$$

the compatibility relation

$$\epsilon_r = (r\epsilon_\theta)', \quad (12)$$

and generalized Hooke's law

$$\epsilon_r = \epsilon_r^p + \frac{1}{E} [\sigma_r - \nu(\sigma_\theta + \sigma_z)] + \int_{T_0}^T \alpha dT, \quad (13)$$

$$\epsilon_\theta = \epsilon_\theta^p + \frac{1}{E} [\sigma_\theta - \nu(\sigma_r + \sigma_z)] + \int_{T_0}^T \alpha dT, \quad (14)$$

$$\epsilon_z = \epsilon_z^p + \frac{1}{E} [\sigma_z - \nu(\sigma_r + \sigma_\theta)] + \int_{T_0}^T \alpha dT, \quad (15)$$

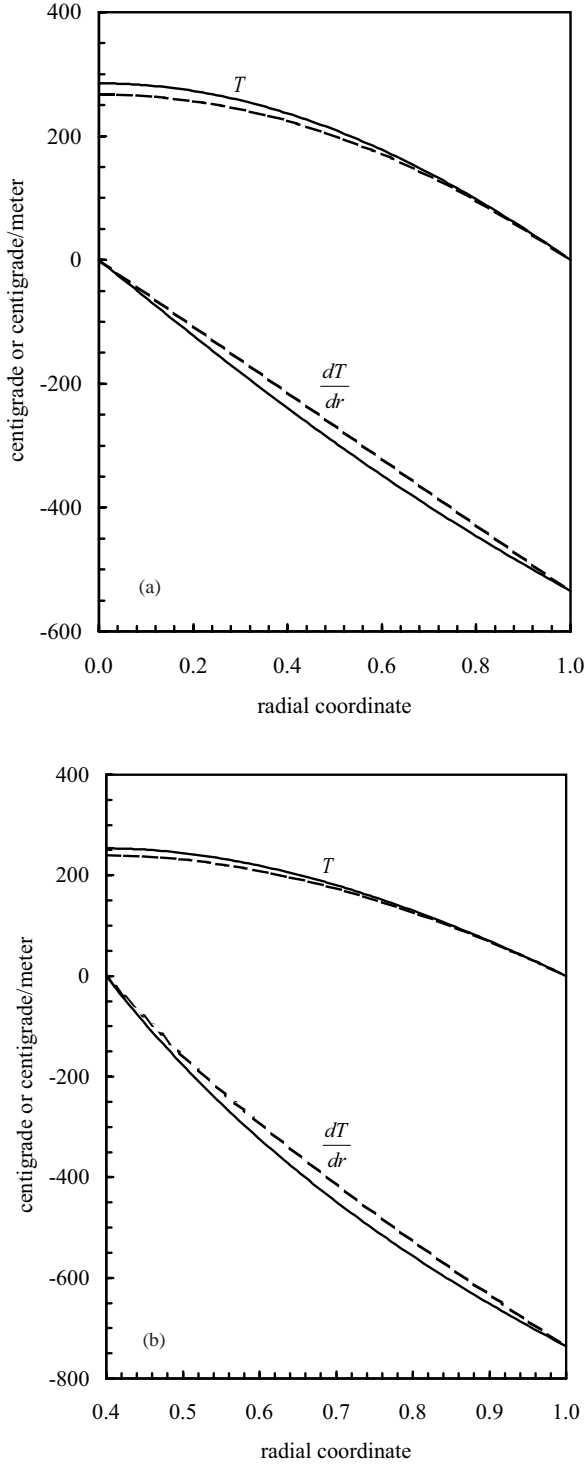


**Figure 2.** The distributions of temperature and temperature gradient in a long (a) uniform heat generating cylinder for  $T_0 = 0$  and  $Q = 6.1$ , (b) uniform heat generating tube of inner radius  $a = 0.4$  for  $T_0 = 0$  and  $Q = 10$ .

are valid both in elastic and in plastic regions. In the equations above,  $\epsilon_j^p$  represents a plastic strain component,  $\nu$  the Poisson ratio, which is almost independent of temperature, and a prime implies differentiation with respect to the nondimensional radial coordinate  $r$ . In a state of generalized plane strain  $\epsilon_z = \epsilon_0 = \text{constant}$  and from Eq. (15) the axial stress is determined as

$$\sigma_z = E(\epsilon_0 - \epsilon_z^p) + \nu(\sigma_r + \sigma_\theta) - E \int_{T_0}^T \alpha dT. \quad (16)$$

At this point, we define the stress function  $Y(r)$  in terms of radial stress as  $Y(r) = r\sigma_r$ , so that from the equation of equilibrium (11)  $\sigma_\theta = Y'(r)$ . The axial stress  $\sigma_z$  is eliminated from Eqs. (13) and (14), and the resulting expressions for the strains in terms of the stress function are substituted in the compatibility relation (12) to obtain the governing equation

$$\begin{aligned} \frac{d^2 Y}{dr^2} + \left[ \frac{1}{r} - \frac{E'}{E} \right] \frac{dY}{dr} - \left[ \frac{1}{r} - \frac{\nu E'}{E(1-\nu)} \right] \frac{Y}{r} = \\ - \frac{E}{(1-\nu^2)r} \left[ \epsilon_\theta^p - \epsilon_r^p + r \frac{d\epsilon_\theta^p}{dr} + r\nu \frac{d\epsilon_z^p}{dr} \right. \\ \left. + r(1+\nu) \frac{d}{dr} \int_{T_0}^T \alpha dT \right], \end{aligned} \quad (17)$$

in which  $E'$  implies  $dE/dr$  and by the use of the chain rule

$$E' = \left[ \frac{dE}{dT} \right] \left[ \frac{dT}{dr} \right]. \quad (18)$$

It should be noted that in the elastic region the plastic strains  $\epsilon_j^p$  and their derivatives vanish and Eq. (17) reduces to the elastic equation

$$\begin{aligned} \frac{d^2 Y}{dr^2} + \left[ \frac{1}{r} - \frac{E'}{E} \right] \frac{dY}{dr} - \left[ \frac{1}{r} - \frac{\nu E'}{E(1-\nu)} \right] \frac{Y}{r} = \\ - \frac{E}{(1-\nu)} \frac{d}{dr} \int_{T_0}^T \alpha dT. \end{aligned} \quad (19)$$

Furthermore, for temperature independent properties  $E' = 0$ ,  $E = 1$  and  $\alpha = \alpha_0$  and hence Eq. (19) simplifies to the form

$$r^2 \frac{d^2 Y}{dr^2} + r \frac{dY}{dr} - Y = - \frac{\alpha_0}{1-\nu} r^2 \frac{dT}{dr}, \quad (20)$$

which is the classical plane strain thermoelastic equation of Cauchy-Euler nonhomogeneous type given in advanced textbooks (Uğural and Fenster, 1995).

Equation (17) is to be integrated for the analysis of thermoelastoplastic response as it automatically switches between field equations for elastic and plastic regions. Since the form given by Eq. (17) is not convenient to handle, an alternate form of this equation containing explicit expressions for the plastic strains will be derived next using the deformation theory of plasticity.

For plane strain, the von Mises yield criterion takes the form

$$\sigma_y = \sqrt{\frac{1}{2}[(\sigma_r - \sigma_\theta)^2 + (\sigma_r - \sigma_z)^2 + (\sigma_\theta - \sigma_z)^2]}. \quad (21)$$

According to total deformation theory, the plastic strains are given as

$$\epsilon_r^p = \frac{\epsilon_{EQ}}{\sigma_y} \left[ \sigma_r - \frac{1}{2}(\sigma_\theta + \sigma_z) \right], \quad (22)$$

$$\epsilon_\theta^p = \frac{\epsilon_{EQ}}{\sigma_y} \left[ \sigma_\theta - \frac{1}{2}(\sigma_r + \sigma_z) \right], \quad (23)$$

$$\epsilon_z^p = \frac{\epsilon_{EQ}}{\sigma_y} \left[ \sigma_z - \frac{1}{2}(\sigma_r + \sigma_\theta) \right], \quad (24)$$

where  $\epsilon_{EQ}$  represents the normalized equivalent plastic strain and, based on a Swift-type nonlinear hardening law, it is related to the yield stress  $\sigma_y$  as

$$\sigma_y = \sigma_0(1 + H\epsilon_{EQ})^{1/m}, \quad (25)$$

where  $m$  is a material parameter. Linearly hardening material behavior is obtained by using  $m = 1$ , and the material behaves nonlinearly hardening otherwise. Total strain components are obtained by the superposition of plastic, elastic and thermal parts as before. They become

$$\begin{aligned} \epsilon_r = & \frac{1}{H\sigma_y} \left[ \left( \frac{\sigma_y}{\sigma_0} \right)^m - 1 \right] \left[ \sigma_r - \frac{1}{2}(\sigma_\theta + \sigma_z) \right] \\ & + \frac{1}{E}[\sigma_r - \nu(\sigma_\theta + \sigma_z)] + \int_{T_0}^T \alpha dT, \end{aligned} \quad (26)$$

$$\begin{aligned} \epsilon_\theta = & \frac{1}{H\sigma_y} \left[ \left( \frac{\sigma_y}{\sigma_0} \right)^m - 1 \right] \left[ \sigma_\theta - \frac{1}{2}(\sigma_r + \sigma_z) \right] \\ & + \frac{1}{E}[\sigma_\theta - \nu(\sigma_r + \sigma_z)] + \int_{T_0}^T \alpha dT, \end{aligned} \quad (27)$$

$$\begin{aligned} \epsilon_z = \epsilon_0 = & \frac{1}{H\sigma_y} \left[ \left( \frac{\sigma_y}{\sigma_0} \right)^m - 1 \right] \left[ \sigma_z - \frac{1}{2}(\sigma_r + \sigma_\theta) \right] \\ & + \frac{1}{E}[\sigma_z - \nu(\sigma_r + \sigma_\theta)] + \int_{T_0}^T \alpha dT. \end{aligned} \quad (28)$$

Some algebraic manipulations are necessary in order to collect the derivative of  $\sigma_\theta$  as it contains the second order derivative of  $Y$ . First, the derivative of the yield stress  $\sigma_y$  is written in the form

$$\frac{d\sigma_y}{dr} = N_1 \frac{d\sigma_r}{dr} + N_2 \frac{d\sigma_z}{dr} + N_3 \frac{d\sigma_\theta}{dr}, \quad (29)$$

where

$$N_1 = \frac{2\sigma_r - \sigma_\theta - \sigma_z}{2\sigma_y}, \quad (30)$$

$$N_2 = \frac{2\sigma_z - \sigma_r - \sigma_\theta}{2\sigma_y}, \quad (31)$$

$$N_3 = \frac{2\sigma_\theta - \sigma_r - \sigma_z}{2\sigma_y}. \quad (32)$$

Then Eq. (28) is differentiated with respect to the radial coordinate  $r$  and Eq. (29) is taken into account to obtain

$$\begin{aligned} \frac{d\sigma_z}{dr} = & \frac{1}{N_7} \left[ \frac{H\sigma_y}{E^2} [\sigma_z - \nu(\sigma_r + \sigma_\theta)] \frac{dE}{dr} \right. \\ & - H\sigma_y \frac{d}{dr} \int_{T_0}^T \alpha dT + m \left( \frac{\sigma_y}{\sigma_0} \right)^{m+1} N_2 \frac{d\sigma_0}{dr} \\ & \left. + N_8 \frac{d\sigma_r}{dr} + N_9 \frac{d\sigma_\theta}{dr} \right], \end{aligned} \quad (33)$$

in which the following variables have just been defined

$$N_4 = (m-1) \left( \frac{\sigma_y}{\sigma_0} \right)^m + 1, \quad (34)$$

$$N_5 = \frac{1}{2} \left[ \left( \frac{\sigma_y}{\sigma_0} \right)^m + \frac{2H\nu}{E} \sigma_y - 1 \right], \quad (35)$$

$$N_6 = \left( \frac{\sigma_y}{\sigma_0} \right)^m + \frac{H}{E} \sigma_y - 1, \quad (36)$$

$$N_7 = N_2^2 N_4 + N_6, \quad (37)$$

$$N_8 = N_5 - N_1 N_2 N_4, \quad (38)$$

$$N_9 = N_5 - N_2 N_3 N_4, \quad (39)$$

Substituting the total strains in the compatibility relation (12) and employing the relations (29) and (33) results in

$$r \left[ 1 + \frac{N_9}{N_7} \right] \frac{d}{dr} \int_{T_0}^T \alpha dT - \frac{r}{E^2} [\sigma_\theta - \nu(\sigma_r + \sigma_z) + \frac{N_9}{N_7} [\sigma_z - \nu(\sigma_r + \sigma_\theta)]] \frac{dE}{dr} - \frac{mr}{H \sigma_0} \left[ N_3 + \frac{N_2 N_9}{N_7} \right] \left( \frac{\sigma_y}{\sigma_0} \right)^m \frac{d\sigma_0}{dr} + \left\{ \frac{1 + \nu}{E} + \frac{3}{2H \sigma_y} \left[ \left( \frac{\sigma_y}{\sigma_0} \right)^m - 1 \right] \right\} (\sigma_\theta - \sigma_r) - \frac{r}{H \sigma_y} \left[ N_{11} + \frac{N_8 N_9}{N_7} \right] \frac{d\sigma_r}{dr} + \frac{r}{H \sigma_y} \left[ N_{10} - \frac{N_9^2}{N_7} \right] \frac{d\sigma_\theta}{dr} = 0, \quad (40)$$

where

$$N_{10} = N_3^2 N_4 + N_6, \quad (41)$$

$$N_{11} = N_5 - N_1 N_3 N_4. \quad (42)$$

If all stresses are expressed in terms of the stress function using  $\sigma_r = Y/r$ ,  $\sigma_\theta = Y'$ , then Eq. (40) can be cast into the general form

$$\frac{d^2 Y}{dr^2} = F(r, Y, \frac{dY}{dr}). \quad (43)$$

The substitution of the axial stress  $\sigma_z$  on the right-hand side of this equation is achieved by the use of Eq. (16). In the plastic region a nonlinear iteration is to be carried out for this purpose. Equation (43) constitutes a nonlinear 2-point boundary value problem and can be solved numerically, subject to the following boundary conditions

$$Y(a) = 0 \text{ and } Y(1) = 0 \text{ for } a \geq 0. \quad (44)$$

Note that while this relation holds for both  $a = 0$  and  $a > 0$ ; in the case  $a = 0$ :  $\sigma_r(0) = Y'(0)$  whereas for  $a > 0$  then  $\sigma_r(a) = Y(a)/a$ . For accurate integration of Eq. (43), a nonlinear shooting method using Newton iterations with numerically approximated tangents is used. To this end we define 2 new variables as  $\phi_1(r) = Y$  and  $\phi_2(r) = dY/dr$  so that one may obtain the system

$$\frac{d\phi_1}{dr} = \phi_2, \quad (45)$$

$$\frac{d\phi_2}{dr} = F(r, \phi_1, \phi_2). \quad (46)$$

Equations (45) and (46) form a system of initial value problems (IVP) and should be solved starting with the initial conditions  $\phi_1(a) = Y(a) = 0$  and  $\phi_2(a) = dY/dr|_{r=a}$ . Since normally the gradient of  $Y$  at  $r = a$  is not known, a Newton iteration scheme is used to obtain the correct value of this gradient by requiring  $\phi_1(b) = Y(b) = 0$ . The double precision

version of the state-of-the-art ODE solver LSODE developed by Hindmarsh (1983) is used for the numerical solution of IVP with the stiff option turned on. An outer iteration loop is performed to determine the value of  $\epsilon_0$  when a free end condition is considered. At each iteration, the problem is solved 3 times using  $\epsilon_0^k$ ,  $\epsilon_0^k + \Delta_\epsilon$  and  $\epsilon_0^k - \Delta_\epsilon$ , respectively, and corresponding net axial forces  $\int \sigma_z dA$  are calculated. A better approximation  $\epsilon_0^{k+1}$  to the constant axial strain is then obtained from

$$\epsilon_0^{k+1} = \epsilon_0^k - \frac{(2\Delta_\epsilon) \int \sigma_z(\epsilon_0^k) dA}{\int \sigma_z(\epsilon_0^k + \Delta_\epsilon) dA - \int \sigma_z(\epsilon_0^k - \Delta_\epsilon) dA}, \quad (47)$$

where  $\Delta_\epsilon$  stands for a small increment of the order  $\epsilon_0^k/100$ . Equation (47) approaches  $\epsilon_0$  in the direction of vanishing net axial force. Starting with a reasonable initial estimate  $\epsilon_0^0$ , this iteration scheme converges to the result with a sufficient accuracy in only a few iterations. Further details of the procedure may be found in Eraslan and Kartal (2004).

### Elastic limits

Assuming constant physical properties, approximate values of the elastic limit heat loads may be evaluated using the elastic equation (20). The general solution is

$$Y(r) = \frac{C_1}{r} + C_2 r - \frac{\alpha_0}{2(1-\nu)} \left[ rT - \frac{I_p(r)}{r} \right], \quad (48)$$

in which  $C_i$  represents an arbitrary integration constant, with  $a$  being the inner radius

$$I_p(r) = \int_a^r T'(\xi) \xi^2 d\xi. \quad (49)$$

Hence, the stress components are determined as

$$\sigma_r = \frac{C_1}{r^2} + C_2 - \frac{\alpha_0}{2(1-\nu)} \left[ T - \frac{I_p(r)}{r^2} \right], \quad (50)$$

$$\sigma_r = -\frac{C_1}{r^2} + C_2 - \frac{\alpha_0}{2(1-\nu)} \left[ T + \frac{I_p(r)}{r^2} \right], \quad (51)$$

$$\sigma_z = 2\nu C_2 + \epsilon_0 - \frac{\alpha_0 T}{1-\nu}. \quad (52)$$

Furthermore, for a generalized plane strain problem the axial strain  $\epsilon_0$  is constant and its value is determined by requiring that the net axial force  $F_z$  must vanish, that is

$$F_z = \int \sigma_z dA = 2\pi \int_a^1 \sigma_z r dr = 0, \quad (53)$$

which gives

$$\epsilon_0 = -2\nu C_2 + \frac{2\alpha_0}{(1-a^2)(1-\nu)} \int_a^1 T(r)r dr. \quad (54)$$

The analytical temperature distributions given by Eqs. (9) and (10) accompany the above solution for cylinders and tubes, respectively.

For a cylinder with fixed ends ( $\epsilon_0 = 0$ ) having the boundary conditions  $\sigma_j(0) \rightarrow finite$  and  $\sigma_r(1) = 0$ , the nondimensional elastic limit heat load  $Q = Q_1$  is determined by the use of yield condition (21) as

$$Q_1 = \frac{16(1-\nu)}{3-2\nu}. \quad (55)$$

If the ends are free, the elastic limit simplifies to

$$Q_1 = 8(1-\nu), \quad (56)$$

For tubes with fixed and free ends the elastic limits are evaluated respectively as

$$Q_1 = 8(1-a^2)(1-\nu)/\sqrt{D}, \quad (57)$$

where

$$D = (1-a^2)^2\{3-\nu(3-\nu)-2a^2[3-\nu(7-3\nu)]+a^4[7-3\nu(5-3\nu)]\}+4a^2(1-a^2)\ln a\{3-\nu+a^4(1-\nu)(5-6\nu)-2a^2[2-\nu(4-\nu)]\}+16a^4(\ln a)^2[1-a^2(1-\nu)+a^4(1-\nu)^2], \quad (58)$$

and

$$Q_1 = \frac{2(1-a^2)(1-\nu)}{1/4-a^2+3/4a^4-a^4\ln a}. \quad (59)$$

In deriving the above limits (57) and (59), traction free boundary conditions:  $\sigma_r(a) = \sigma_r(1) = 0$  have been used. These limits may form practical test cases for the present model.

Taking the Poisson's ratio  $\nu = 0.3$ , elastic limit heat loads for cylinders and tubes of different inner radius are determined by virtue of Eqs. (55), (56), (57), and (59). These limits are referred to as constant physical properties (CPP) and are compared to those computed using temperature dependent properties (VPP) in Table 1. The symbols (c), (i), and (o) in this table stand for center, inner surface, and outer surface, respectively, and indicate the location of yielding. As seen in Table 1, yielding commences at the center in uniform heat generating long cylinders irrespective of the end condition. Since the uniaxial yield limit  $\sigma_0$  decreases rapidly with increasing temperatures (see Figure 1), the solutions with temperature dependent properties predict lower limits, as expected. The inner surface of tubes with fixed ends is critical and plastic deformation first begins at this location. Again VPP solutions predict lower elastic limits. Interesting deformation behavior occurs in tubes with free ends. Analytical CPP solutions indicate that the outer surface is critical and plastic deformation first begins there when  $Q$  reaches

**Table 1.** Elastic limit heat loads.

$a$	Fixed End		Free End	
	CPP	VPP	CPP	VPP
0	4.6667 (c)	3.99945 (c)	5.6000 (o)	5.32571 (o)
0.1	4.0352 (i)	3.528935 (i)	5.7677 (o)	4.788243 (i)
0.2	4.6258 (i)	4.042573 (i)	6.2870 (o)	5.62087 (i)
0.3	5.5963 (i)	4.887427 (i)	7.2458 (o)	6.90417 (o)
0.4	7.1519 (i)	6.242368 (i)	8.8650 (o)	8.45426 (o)
0.5	9.7595 (i)	8.51398 (i)	11.641 (o)	11.11075 (o)

the critical values given in Table 1. However, for tubes having nondimensional inner radii 0.1 and 0.2, VPP computations predict that plastic deformation commences at the inner surface.

The stresses in a tube of  $a = 0.2$  with free ends are plotted in Figures 3(a) and (b). Figure 3(a) shows the results of analytical (dots) and numerical (solid lines) CPP calculations corresponding to the limit  $Q = 6.2870$ . Analytical and numerical solutions agree perfectly, allowing one to assess the accuracy of the computational procedure. In fact, in all calculated, both solutions agree to at least 8 significant digits. The nondimensional yield variable  $\phi$  in this figure is calculated from

$$\phi = \frac{1}{\sigma_0} \sqrt{\frac{1}{2} [(\sigma_r - \sigma_\theta)^2 + (\sigma_r - \sigma_z)^2 + (\sigma_\theta - \sigma_z)^2]}, \tag{60}$$

which corresponds to the yield stress  $\sigma_y$  in the plastic core. Note that  $\phi = 1$  at the plastic-elastic border and  $\phi < 1$  in the elastic region. As seen in Figure 3(a),  $\phi(b) = 1$ , indicating the location of plastic deformation. Figure 3(b), on the other hand, is based on numerical VPP calculations at  $Q = 5.62087$ . Following the variation of  $\phi$ , it is seen that the stress state is critical at the inner surface, in contrast to CPP data, and the tube begins to plasticize at this location.

### Sample Computations

In this section, the results of elastoplastic computations considering variable physical properties (VPP) for different problems are presented and compared to those of constant physical property (CPP) predictions. The Poisson's ratio is  $\nu = 0.3$ , and in all the figures dashed lines show CPP results, while solid lines show VPP corresponding to the same values of material parameters ( $H$  and  $m$ ) and the heat load  $Q$ .

As seen in Table 1, the heat generating cylinder with fixed ends becomes partially plastic for  $Q > Q_e = 3.99945$  irrespective of the hardening parameters  $H$  and  $m$ . Plastic deformation commences at the center when  $Q = 3.99945$  and the plastic core formed here propagates toward the edge as the heat load is increased. Under the load  $Q = Q_S$  the stress state at the surface becomes critical so that another plastic region forms there. The value of  $Q_S$  is dependent mainly on parameters  $H$  and  $m$ , which describe the nonlinear hardening path. For  $Q > Q_S$ , the

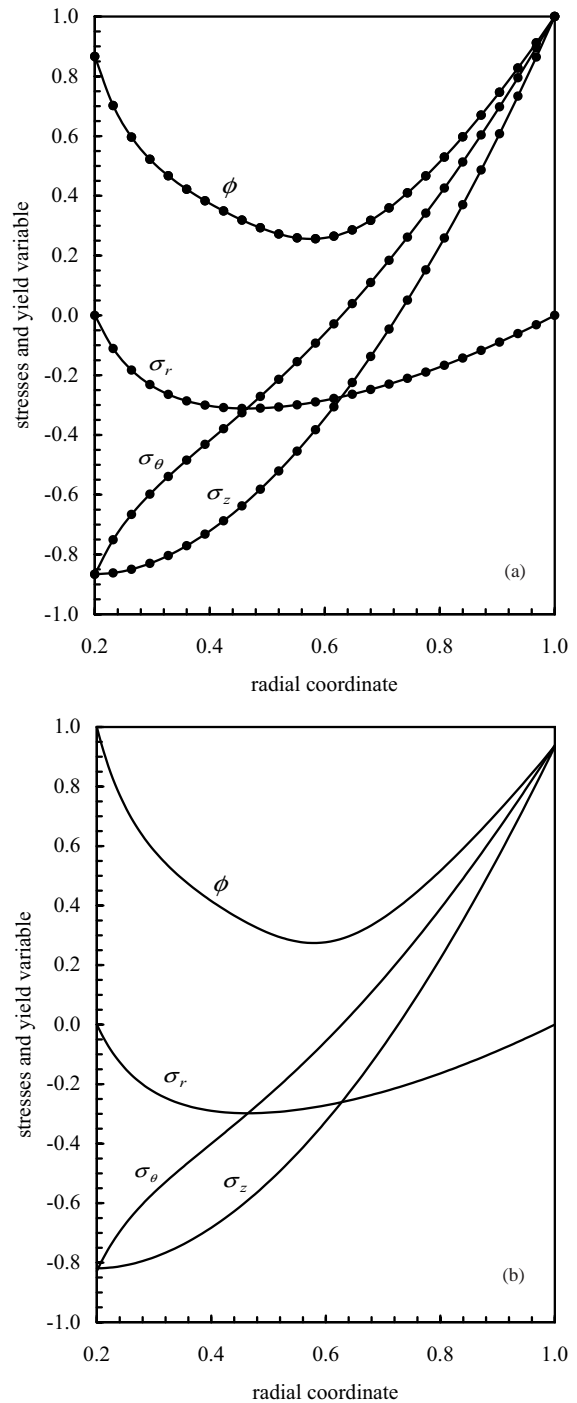


**Figure 3.** The elastic stresses in a tube with free ends having an inner radius of  $a = 0.2$ . (a) Comparison of analytical (dots) and numerical (dashed lines) solutions keeping physical properties constant under elastic limit heat load  $Q_e = 6.2870$ , (b) solution using temperature dependent physical properties at  $Q_e = 5.62087$ .

2 plastic regions propagate toward each other until the cylinder becomes fully plastic. Taking  $H = 0.25$  and  $m = 0.75$  and assigning  $Q = 6.1 > Q_S$  the stresses, the nondimensional yield variable  $\phi$  (Eq. 60) and the radial displacement are calculated and plotted in Figure 4(a). The dimensionless radius  $r_{ep}$  in this figure and in the following ones indicates an elastic-plastic border and subscripts  $ep1$  and  $ep2$  imply primary and secondary plastic formations, respectively. As seen in Figure 4(a), the cylinder is composed of 3 different regions: an inner plastic region in  $0 \leq r \leq r_{ep1}$ , an elastic region in  $r_{ep1} \leq r \leq r_{ep2}$ , and an outer plastic region in  $r_{ep2} \leq r \leq b$ . The elastic-plastic border radii  $r_{ep1}$  and  $r_{ep2}$  are estimated as 0.78075 and 0.93903, respectively. The CPP calculations, however, predict only one plastic region, and a broader elastic region, as shown in Figure 4(a). The cylinder is composed of a plastic core in  $0 \leq r \leq r_{ep1}$  and an elastic ring in  $r_{ep1} \leq r \leq b$ . The elastic-plastic border radius is determined as  $r_{ep1} = 0.56803$ . Figure 4(b) shows the residual stresses and displacement upon removal of the load  $Q = 6.1$ . They are calculated by subtracting the stresses and displacement corresponding to unrestricted elastic behavior from elastic-plastic ones at the same load parameter. Of course, this calculation procedure holds true only when the residual stresses do not exceed the yield limit (Eraslan and Argeso, 2005a). In this figure, the nondimensional stress components are designated by  $\sigma_j^0$  and displacement by  $u^0$  to imply stand-still. The yield variable  $\phi^R$  is calculated from Eq. (60) with  $\sigma_j$  replaced by  $\sigma_j^0$ . Since  $\phi^R < 1$ , unloading occurs elastically and reversed plastic flow (secondary plastic flow) does not take place.

The partially plastic stress state in the heat generating cylinder with free ends under the load  $Q = 7.6$  is depicted in Figure 5(a). The material parameters used are  $H = 0.25$  and  $m = 1.25$ . The VPP solution predicts 2 plastic regions and an elastic region, whilst the CPP solution predicts an elastic and a plastic region, as shown in Figure 5(a). The elastic-plastic border radii from left to right are calculated as  $r_{ep2} = 0.19049$ ,  $r_{ep1} = 0.82784$ , and  $r_{ep1} = 0.89307$ . The cylinder expands in the axial direction as much as  $\epsilon_0 = 1.0453$ , according to the VPP solution. It is  $\epsilon_0 = 0.97081$  in the CPP calculation. The residual stresses and displacement at stand-still are also calculated and plotted in Figure 5(b). Secondary plastic flow does not take place upon complete removal of the load  $Q = 7.6$ .

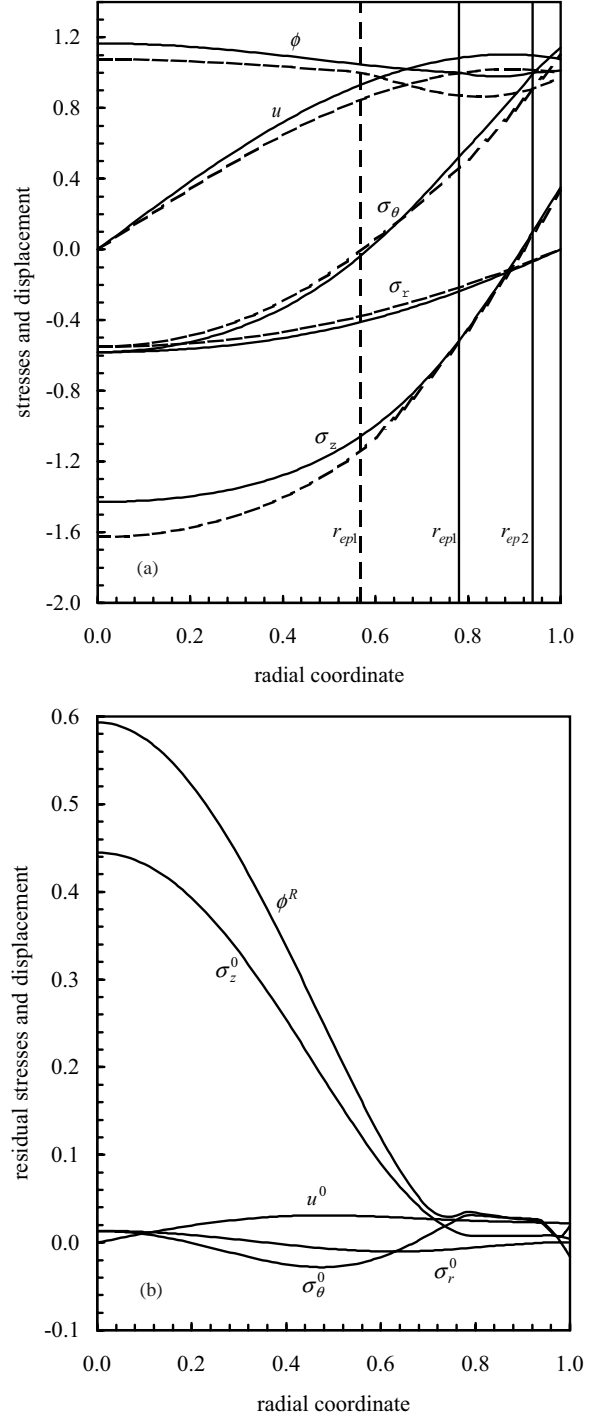


**Figure 4.** (a) Comparison of VPP (solid lines) and CPP (dashed lines) solutions for the thermal stresses and displacement in a partially plastic, nonlinearly hardening cylinder with fixed ends at  $Q = 6.1$  for  $H = 0.25$  and  $m = 0.75$ . (b) The residual stresses based on VPP solution upon complete removal of the heat load.

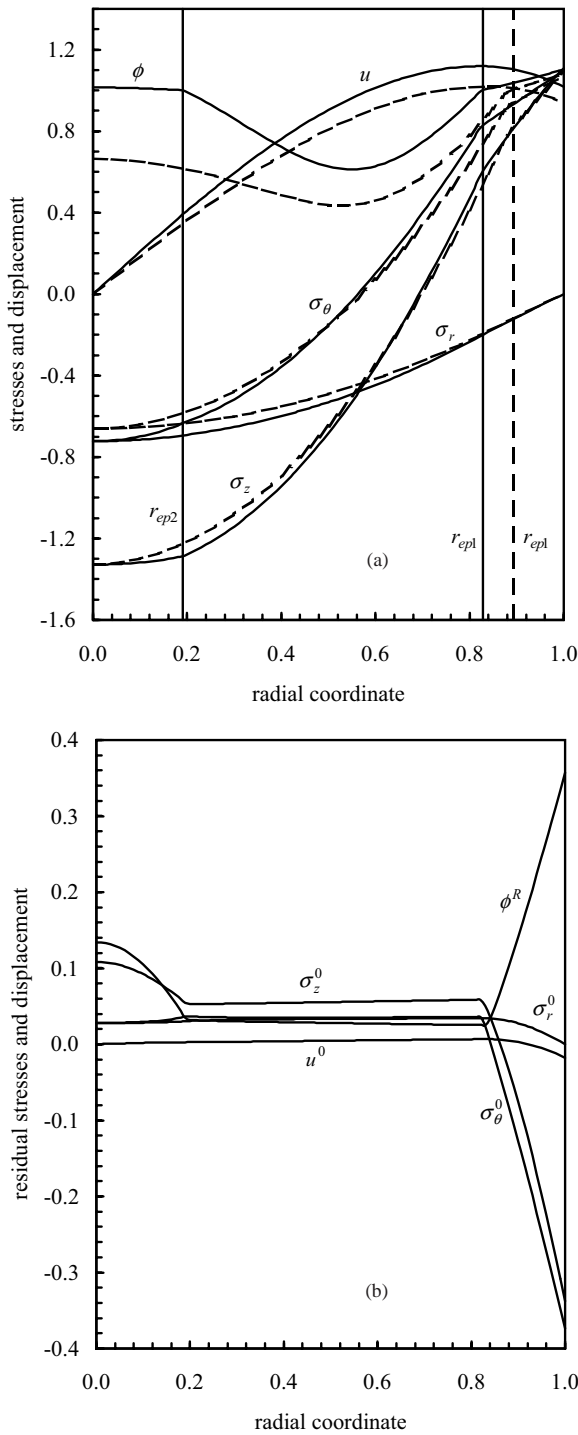


**Figure 5.** (a) Comparison of VPP (solid lines) and CPP (dashed lines) solutions for the thermal stresses and displacement in a partially plastic, nonlinearly hardening cylinder with free ends at  $Q = 7.6$  for  $H = 0.25$  and  $m = 1.25$ . (b) The residual stresses based on VPP solution upon complete removal of the heat load.

Fig 6(a) shows the stresses and displacement in a heat generating partially plastic tube with fixed ends. The bore radius is  $a = 0.4$  and the parameters are  $H = 0.25$ ,  $m = 1.25$  and  $Q = 10$ . Under this load the tube is composed of an inner plastic core in  $0.4 \leq r \leq 0.74577$ , an elastic ring in  $0.74577 \leq r \leq 0.97589$ , and outer plastic zone in  $0.97589 \leq r \leq 1.0$ . The border radius by the CPP solution is  $r_{ep1} = 0.64655$ , which divides the tube into plastic and elastic regions. The plastic strain components shown in Figure 6(b) help to explain how the VPP and CPP elastoplastic responses of the tube differ. The residual stresses and residual displacement at stand-still are shown in Figure 6(c). Unloading occurs elastically on removal of  $Q = 10$ ; however,  $\phi^R(a) \approx 0.72$  is large and secondary plastic flow may take place as the heat load is slightly increased.

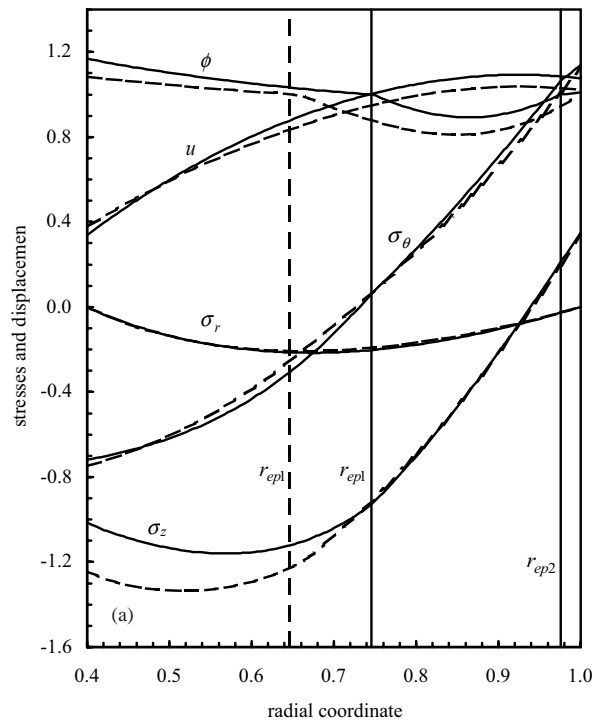


**Figure 6.** (a) Comparison of VPP (solid lines) and CPP (dashed lines) solutions for the thermal stresses and displacement in a partially plastic, nonlinearly hardening tube of  $a = 0.4$  with fixed ends at  $Q = 10$  for  $H = 0.25$  and  $m = 1.25$ . (b) The corresponding plastic strain components. (c) The residual stresses based on VPP solution upon complete removal of the heat load.

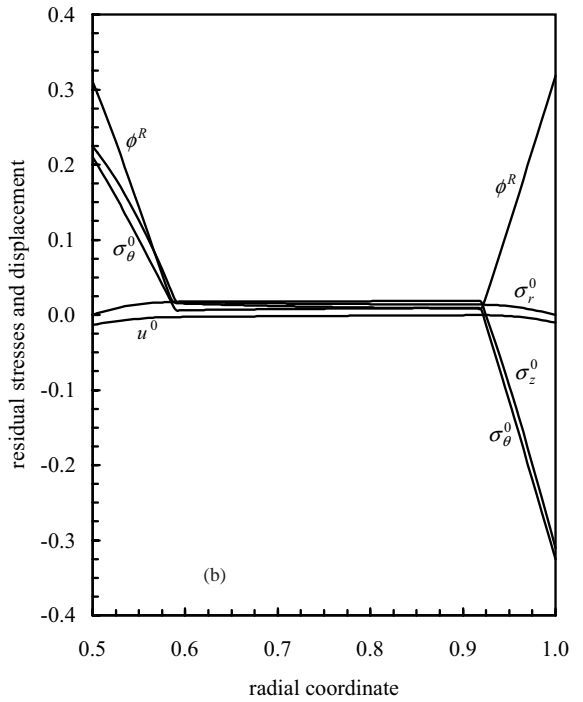
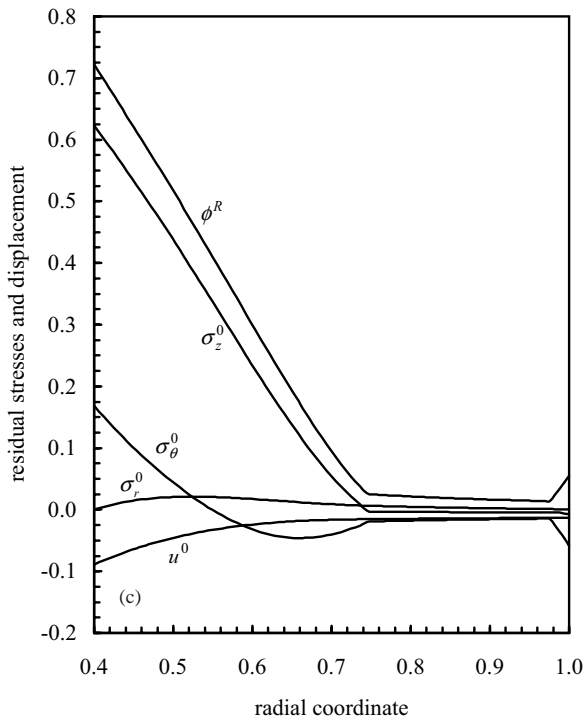
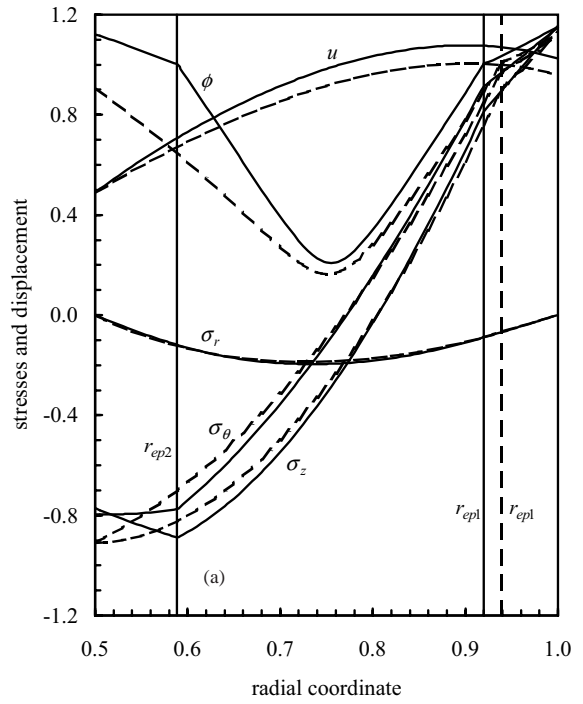
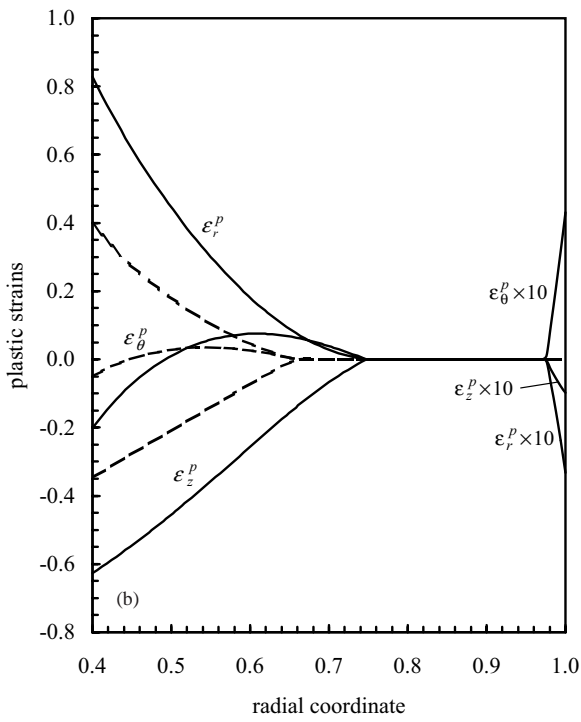


Figure 6. Continued.

Figure 7. (a) Comparison of VPP (solid lines) and CPP (dashed lines) solutions for the thermal stresses and displacement in a partially plastic, nonlinearly hardening tube of  $a = 0.5$  with free ends at  $Q = 16$  for  $H = 0.25$  and  $m = 0.75$ . (b) The residual stresses based on VPP solution upon complete removal of the heat load.

Finally, the elastoplastic deformation behavior of a tube with free ends is studied by considering  $a = 0.5$ ,  $H = 0.25$ ,  $m = 0.75$  and loading with  $Q = 16.0$ . The corresponding stresses are plotted in Figure 7(a). The border radii in this figure, from left to right, are  $r_{ep2} = 0.58831$ ,  $r_{ep1} = 0.91983$ , and  $r_{ep1} = 0.93949$ . The VPP prediction for axial expansion is  $\epsilon_0 = 1.0349$ , while it is 0.97632 by CPP. The residual stresses at stand-still for this tube are shown in Figure 7(b).

### Concluding Remarks

A computational model for the estimation of thermally induced plane strain elastic, partially plastic, fully plastic, and residual stress states and deformations is outlined. This work represents a necessary extension of the authors' previous study (Eraslan and Argeso, 2005a) to include the temperature dependency of the physical properties of the material. The fact that the physical properties of engineering

materials vary considerably with temperature (Figure 1) was the main point motivating this work. The critical differences between constant and variable physical property calculations can clearly be evaluated in the results of this work (Figures 3(a)-(b), 4(a), 5(a), 6(a)-(b), 7(a)). Since, in general, the modulus of elasticity decreases with temperature, the strength of the material to elastically resist thermal loads decreases. As a result, the material fails with respect to plastic deformation under much lower thermal loads than those predicted by CPP solutions (Table 1). The region deformed plastically propagates more rapidly than CPP data because of the fact that the uniaxial yield limit is very sensitive to temperature. Fully plastic stress states are reached at much lower thermal loads and different modes of plasticization may take place. In the light of these critical findings, it can be concluded that the inclusion of temperature dependent physical properties is required in thermal stress calculations in order to obtain more realistic predictions.

### References

- Boley, B.A. and Weiner, J.H., *Theory of Thermal Stresses*, Wiley, New York, 1960.
- Chen, W.F. and Han, D.J., *Plasticity for Structural Engineers*, Springer, New York, 1988.
- Eraslan, A.N., "Thermally Induced Deformations of Elastic-plastic Composite Tubes Subjected to a Nonuniform Heat Source". *Journal of Thermal Stresses* 26, 167-193, 2003.
- Eraslan, A.N., "Von Mises' Yield Criterion and Non-linearly Hardening Rotating Shafts". *Acta Mechanica* 168, 129-144, 2004.
- Eraslan, A.N. and Akis, T., "On the Elastic-plastic Deformation of a Rotating Disk Subjected to a Radial Temperature Gradient". *Mechanics Based Design of Structures and Machines* 31, 529-561, 2003.
- Eraslan, A.N. and Argeso, H., "On the Application of von Mises' Yield Criterion to a Class of Plane Strain Thermal Stress Problems". *Turkish Journal of Engineering and Environmental Sciences* 29, 113-128, 2005a.
- Eraslan, A.N. and Argeso, H., "A Nonlinear Shooting Method Applied to Solid Mechanics: Part 2. Numerical Solution of a Plane Strain Model". *International Journal of Nonlinear Analysis and Phenomena* 2, 31-42, 2005b.
- Eraslan, A.N. and Kartal, M.E., "A Nonlinear Shooting Method Applied to Solid Mechanics: Part 1. Numerical Solution of a Plane Stress Model". *International Journal of Nonlinear Analysis and Phenomena* 1, 27-40, 2004.
- Eraslan, A.N. and Orcan, Y., "Computation of Transient Thermal Stresses in Elastic-Plastic Tubes: Effect of Coupling and Temperature Dependent Physical Properties". *Journal of Thermal Stresses* 25, 559-572, 2002.
- Eraslan, A.N. and Orcan, Y., "Thermoplastic Response of a Linearly Hardening Cylinder Subjected to Nonuniform Heat Source and Convective Boundary Condition". *Mechanics Based Design of Structures and Machines* 32, 133-164, 2004.
- Eraslan, A.N., Sener, E. and Argeso, H., "Stress Distributions in Energy Generating Two-layer Tubes Subjected to Free and Radially Constrained Boundary Conditions". *International Journal of Mechanical Sciences* 45, 469-496, 2003.
- Hindmarsh, A.C., "ODEPACK: A Systematized Collection of ODE Solvers". In: *Scientific Computing* (Stepleman RS, ed.) North Holland, Amsterdam, 1983.
- Johnson, W. and Mellor, P.B., *Engineering Plasticity*, Van Nostrand Reinhold, London, 1973.
- Orcan, Y., "Thermal Stresses in a Heat Generating Elastic-plastic Cylinder with Free Ends". *International Journal of Engineering Science* 32, 883-898, 1994.

Orcan, Y. and Eraslan, A.N., "Thermal Stresses in Elastic-plastic Tubes with Temperature Dependent Mechanical and Thermal Properties". *Journal of Thermal Stresses* 24, 1097-1113, 2001.

Orcan, Y. and Gulgec, M., "Elastic-plastic Deformation of a Tube with Free Ends Subjected to Internal Heat Generation". *Turkish Journal of Engineering and Environmental Science* 25, 1-10, 2001.

Rees, D.W.A., *The Mechanics of Solids and Structures*, McGraw-Hill, New York, 1990.

Timoshenko, S. and Goodier, J.N., *Theory of Elasticity*, 3rd ed. McGraw-Hill, New York, 1970.

Uğural, A.C. and Fenster, S.K., *Advanced Strength and Applied Elasticity*, 3rd ed. Prentice-Hall International, London, 1995.